Journal of Power Sources 220 (2012) 103–107

Contents lists available at SciVerse ScienceDirect

Journal of Power Sources

journal homepage: www.elsevier.com/locate/jpowsour

Short communication

Nanoparticle Li_2FeSiO_4 as anode material for lithium-ion batteries

Yang Xu, Yajuan Li*, Suqin Liu, Hongliang Li, Younian Liu

College of Chemistry and Chemical Engineering, Central South University, 932 Lu Shan Road, Changsha 410083, Hunan, China

HIGHLIGHTS

- Nano-sized Li_2FeSiO_4 was synthesized by sol–gel method using as an anode material for lithium ion batteries.
- The Li_2FeSiO_4 anodes delivered an initial discharge capacity of 880 mA h g^{-1}.
- The anodes exhibited excellent cycling and rate performance.
- *Ex-situ* XRD, XPS and cyclic voltammograms have been analyzed and interpreted to conjecture the reaction mechanism.

ARTICLE INFO

Article history:
Received 20 April 2012
Received in revised form
16 June 2012
Accepted 31 July 2012
Available online 9 August 2012

Keywords:
Lithium-ion battery
Lithium iron silicate
Anode material
Sol–gel process
Citric acid

ABSTRACT

Nano-sized Li_2FeSiO_4 particles are successfully synthesized by sol–gel method using as anode materials for lithium-ion batteries. The X-ray diffraction pattern confirms the monoclinic structure with a space group of $P2_1$. The TEM images show that the primary size of Li_2FeSiO_4 nanoparticle is 20–40 nm. The Li_2FeSiO_4 nanoparticle is coated by a very thin film of amorphous carbon, the carbon content is 10.06%. The Li_2FeSiO_4 electrode delivers an initial discharge capacity of 880 mA h g^{-1}, which is much higher than graphitic anodes. The specific discharge capacity of the Li_2FeSiO_4 electrode at 500 mA g^{-1} is 235 mA h g^{-1}. The electrode delivers a specific discharge capacity of about 449 mA h g^{-1} at the current density of 100 mA g^{-1} even after 173 cycles. The electrochemical procedures of the Li_2FeSiO_4 electrode are emphasized by *ex-situ* XRD, XPS and cyclic voltammograms.

1. Introduction

Since the commercial lithium-ion batteries (LIBs) were developed for portable electronic devices in the 1990s, it has been considered as an attractive power source for a wide variety of applications. Low initial irreversible capacity loss and high cycling stability have considered as the basic demands of advanced anode materials for LIBs. Graphitic carbon was firstly used as anode materials for LIBs by Sony, although such materials offered a lower theoretical capacity of 372 mA h g^{-1} [1]. To solve the capacity limitations, reduce the cost and improve energy density, cycling life and high-rate capability, many efforts are being made to search alternative anode materials for LIBs [2–6]. Li alloy based anodes (e.g. Li–Sn) has been studied due to its high theoretical capacity compared to commercial graphite [2]. However, alloy-based anode has a problem with severe capacity fading due to the large volume variation during alloying/dealloying process [7–9]. Poizot et al. reported that the nano-sized 3d transition-metal oxides electrodes (e.g. CoO) could get a capacity of 700 mA h g^{-1} and 100% capacity retention. The reaction mechanism differs from the conventional Li insertion/deinsertion or Li-alloying mechanism; it consists of the reversible reduction of the transition mental oxides to the metallic state, coupled with the formation and decomposition of Li_2O [9]. However, this kind of anode material has high irreversible capacity and working potential, the cycling stability is also not very good due to the low diffusion coefficient and active materials loss contact with current collector during cycling. It is necessary to explore an anode material with high capacity and capacity retention.

Utilization of cathode materials into negative electrodes is a hotspot in today's research. Such as $LiFePO_4$, which has a theoretical capacity of 170 mA h g^{-1} with a flat voltage plateau at 3.4 V versus Li when used as cathode. Surprisingly, $LiFePO_4$ exhibited an initial capacity of ~620 mA h g^{-1} and excellent coulombic efficiency value of 99% while tested as anode [10]. Similar researches on $FePO_4$ [11] and Li_2MnSiO_4 [12] have also been reported.

Li_2FeSiO_4 have been explored by Nytén et al. as a cathode material, which has a theoretical capacity of 166 mA h g^{-1} upon

* Corresponding author. Tel./fax: +86 731 8887 9850.
E-mail address: yajuanli@csu.edu.cn (Y. Li).

0378-7753/$ – see front matter © 2012 Elsevier B.V. All rights reserved.
http://dx.doi.org/10.1016/j.jpowsour.2012.07.130

the removal of 1 Li-ion and a voltage plateau at 2.85 V (versus Li) [13]. In this paper, we report lithium orthosilicate material (e.g. Li_2FeSiO_4) as a promising candidate anode material for lithium rechargeable batteries due to its low cost, environmental benignity, high theoretical capacity and ease to prepare. Despite Li_2FeSiO_4 being briskly investigated as a positive electrode [13–16], the anode materials of Li_2FeSiO_4 have not been reported. Surprisingly, a higher initial capacity has been exhibited by Li_2FeSiO_4 anode, which is times higher than the capacity of the corresponding Li_2FeSiO_4 cathode.

2. Experimental

2.1. Synthesis of Li_2FeSiO_4

Sol-gel method based on citric acid was employed to prepare the Li_2FeSiO_4 powers. Analytical grades of $Fe(NO_3)_3\cdot 9H_2O$, $CH_3COOLi\cdot 2H_2O$, $(C_2H_5O)_4Si$, and citric acid were used as the starting materials in a molar ratio of 1:2:1:2 and dissolved in distilled water. $Fe(NO_3)_3\cdot 9H_2O$ solution was firstly added into the solution of $CH_3COOLi\cdot 2H_2O$, then, the saturated aqueous solution of citric acid and $(C_2H_5O)_4Si$ were slowly added to the above solution under magnetic stirring in turn. After stirring for 3 h in the room temperature, the mixed solution was evaporated at 80 °C under continuous stirring to get a wet gel. The resulting wet gel was dried in an oven and then calcined at 600 °C for 10 h in a flowing argon atmosphere.

2.2. Measurements

The working electrode membrane was fabricated with 80 wt % of the active material, 10 wt% acetylene black and 10 wt% polytetrafluoroethylene (PTFE) binder. It was pressed on a stainless steel mesh current collector (Φ10 mm) at 15 MPa and drying at 383 K for 12 h in a vacuum oven. CR2016 coin cells were assembled in an argon-filled glove box using lithium foil as counter electrode, polypropylene film (Celgard 2300) as separator, and 1 M $LiPF_6$ in a mixture of EC–DMC–DEC (volume ratio of 1:1:1) as the electrolyte. The coin cells were galvanostatically cycled between 0 and 3.0 V by Land CT2001A battery testing system at room temperature. Cyclic voltammetry (CV) measurements were performed on a CHI660D (Shanghai China) workstation with a scan rate of 0.2 mV s^{-1} between 0 and 3.0 V.

The crystalline phases were identified with XRD (*D*max/2550VB, Rigaku) with Cu Kα radiation. Morphological features were observed with JEM-6360-LV scanning electron microscope (SEM), JEM-2010 transmission electron microscope (TEM) and high resolution transmission electron microscope (HRTEM). The content of carbon was determined by elementary analysis (Vario EL III). X-ray photoelectron spectroscopy (XPS) was performed with a K-Alpha 1063 type analyzer with monochromatic Al Kα radiation (Electrophysics, Britain) to measure the chemical or electronic state of different element in the surface. The cycled cells were disassembled in a glove box to recover the electrode materials, which was then

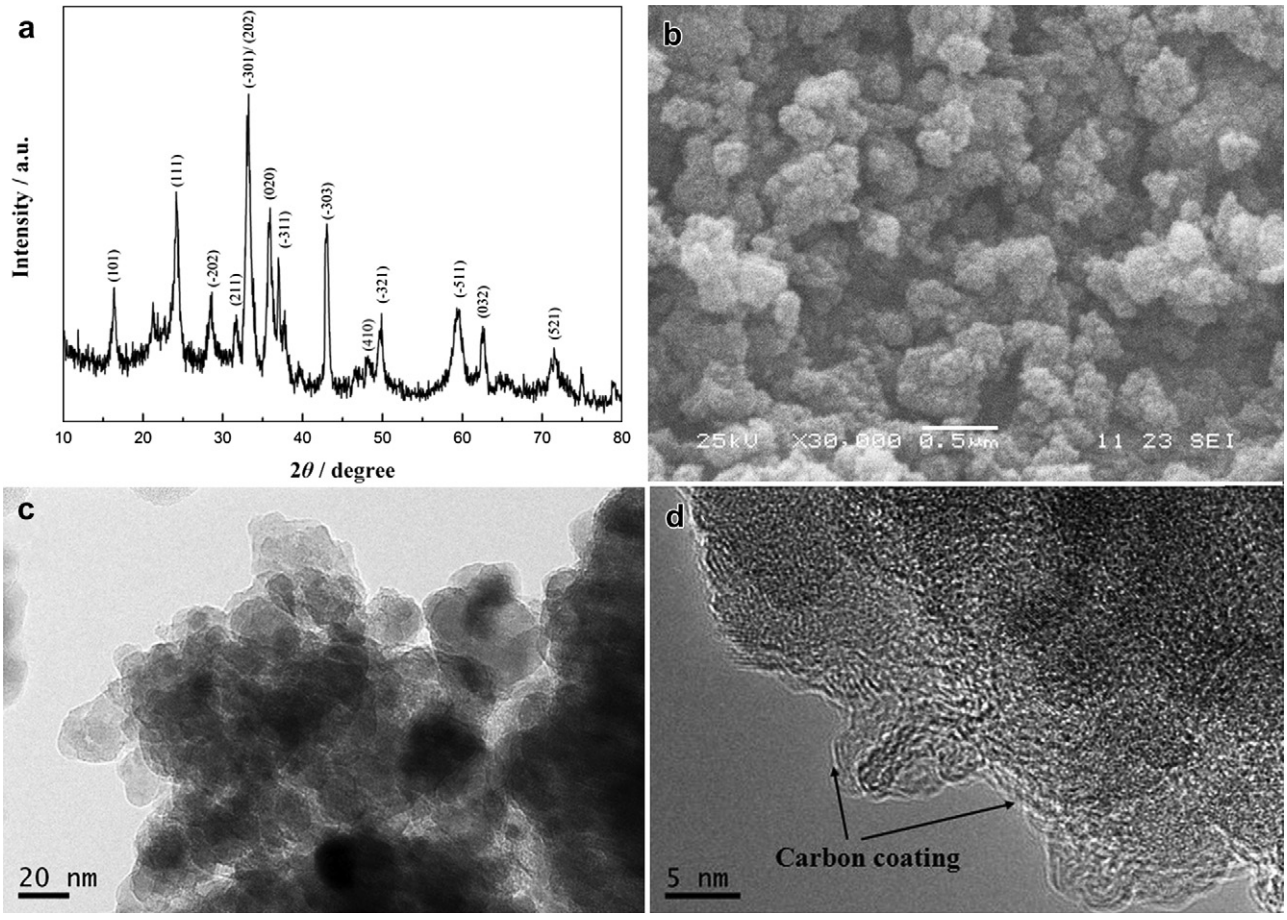

Fig. 1. Characterization of the as-prepared Li_2FeSiO_4: (a) XRD pattern; (b) SEM image; (c) TEM image; (d) HRTEM image.

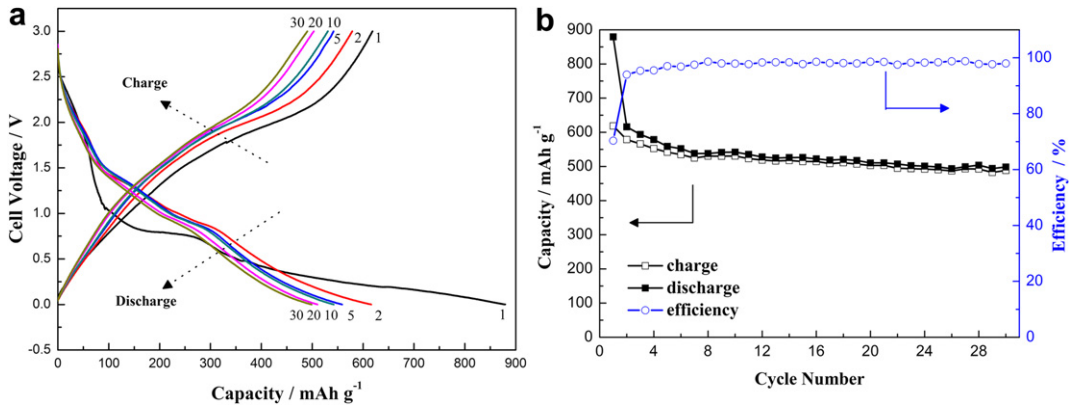

Fig. 2. (a) The discharge–charge voltage profiles and (b) the cycling profiles of Li_2FeSiO_4 electrode between 0 and 3.0 V at a current density of 50 mA g^{-1}.

rinsed thoroughly with a DMC solution to remove electrolyte traces before characterized by XRD and XPS.

3. Results and discussion

3.1. Characterization of the as-prepared Li_2FeSiO_4

The XRD pattern of the as-prepared Li_2FeSiO_4 is shown in Fig. 1a, which can be indexed to a monoclinic structure with a space group of $P2_1$ [15]. The calculated lattice parameters are a = 8.2346 Å, b = 5.0172 Å, c = 8.2251 Å, and β = 99.052°, which are close to those reported by Nishimura et al. [17]. The XRD pattern shows the well-defined sharp intense reflections, which indicate the highly crystalline nature of the as-prepared Li_2FeSiO_4. Fig. 1b shows an SEM image of the as-prepared Li_2FeSiO_4, which demonstrates that the powder is composed of aggregated nanoparticles. The TEM image shown in Fig. 1c illustrates that the primary crystallite size of these nanoparticles is 20–40 nm. Fig. 1d shows an HRTEM image of the Li_2FeSiO_4 nanoparticle. It is shown that the Li_2FeSiO_4 nanoparticle was coated by a very thin film of amorphous carbon. The elementary analysis of carbon content for Li_2FeSiO_4 nanoparticle is 10.06%.

3.2. Electrochemical performance

The electrochemical performance of Li_2FeSiO_4 electrode were evaluated by galvanostatic discharge–charge cycling in the voltage between 0 and 3.0 V at a current density of 50 mA g^{-1} up to 30 cycles at room temperature, the voltage and cycling profiles are shown in Fig. 2. For clarity, only representative cycles of the curves are shown. The open-circuit voltage (OCV) of the assembled cell is about 2.8 V. As shown in Fig. 2a, during the first discharge, a wide voltage plateau at about 0.8 and 0.2 V can be observed, the first discharge capacity is 880 mA h g^{-1}, which is much higher than commercially graphitic anode. The first charge profile of Li_2FeSiO_4 electrode shows a strong polarization of ~1.0 V followed by a voltage plateau at about 2.0 V, the first charge capacity is 618 mA h g^{-1}. The irreversible capacity loss is about 29.8%, which can be mainly attributed to the possible irreversible reduction on the electrode, electrolyte decomposition and inevitable formation of an SEI layer [3–6]. The relative work relating to the initial loss is now in progress in our group. During the second discharge–charge cycle, discharge voltage plateaus appear at 0.8 and 1.3 V, respectively. The discharge capacity drastically reduces from 880 to 616 mA h g^{-1}. Interestingly, the high specific capacity Li_2FeSiO_4 electrode exhibits remarkable cyclic reversibility with an acceptable fade in capacity values, the discharge capacity retains 498 mA h g^{-1}after 30 cycles (Fig. 2b). The decay of specific capacity of the Li_2FeSiO_4 electrode is ascribable to the factors such as

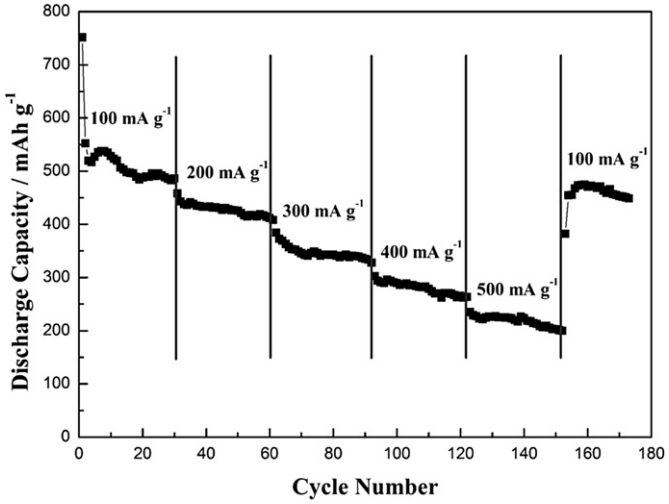

Fig. 3. Cycling profiles of Li_2FeSiO_4 electrode at various current densities.

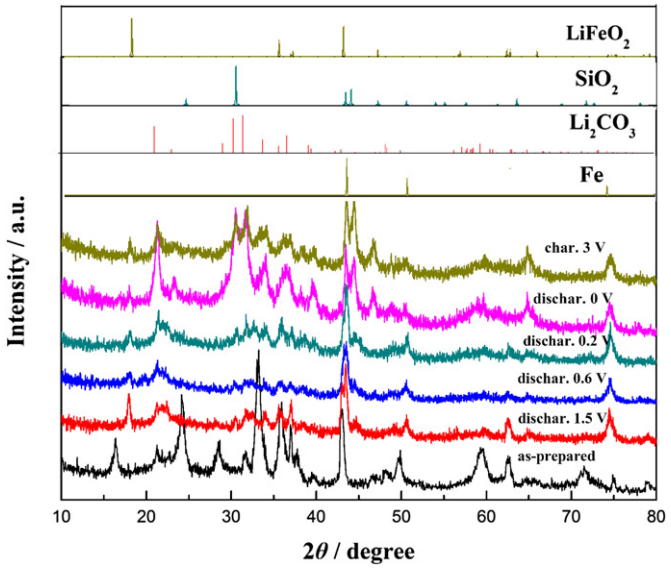

Fig. 4. XRD patterns of Li_2FeSiO_4 electrode discharged and charged to various voltages in the initial cycle (the standard XRD patterns of Fe, Li_2CO_3, SiO_2 and $LiFeO_2$ are also shown for reference).

structural variations, particle pulverization and loss contact with the conductive binder [10]. Similarly, the coulombic efficiency steadily reaches the values higher than 97.5%.

In order to get full estimation of the electrochemical performance of Li_2FeSiO_4 electrode, the consecutive cycling behaviors at various discharge–charge current densities, measured from 100 to 500 mA g^{-1} in an ascending order, followed by a return to 100 mA g^{-1}, is shown in Fig. 3. The Li_2FeSiO_4 electrode presents good cycling stability at each rate, and reversible capacities were measured to be 552, 458, 384 and 302 mA h g^{-1} at the current density of 100, 200, 300 and 400 mA g^{-1}, respectively. Even at 500 mA g^{-1}, the discharge capacity is 235 mA g^{-1}, it is 43% of the second specific discharge capacity at 100 mA g^{-1}. On returning to 100 mA g^{-1}, the electrode delivers a specific discharge capacity of about 449 mA h g^{-1} even after 173 cycles, indicating that the structure of the material was stable during the cycling.

To confirm the phases during discharge/charging, *ex-situ* XRD of Li_2FeSiO_4 was investigated (Fig. 4). As the anode is discharged to

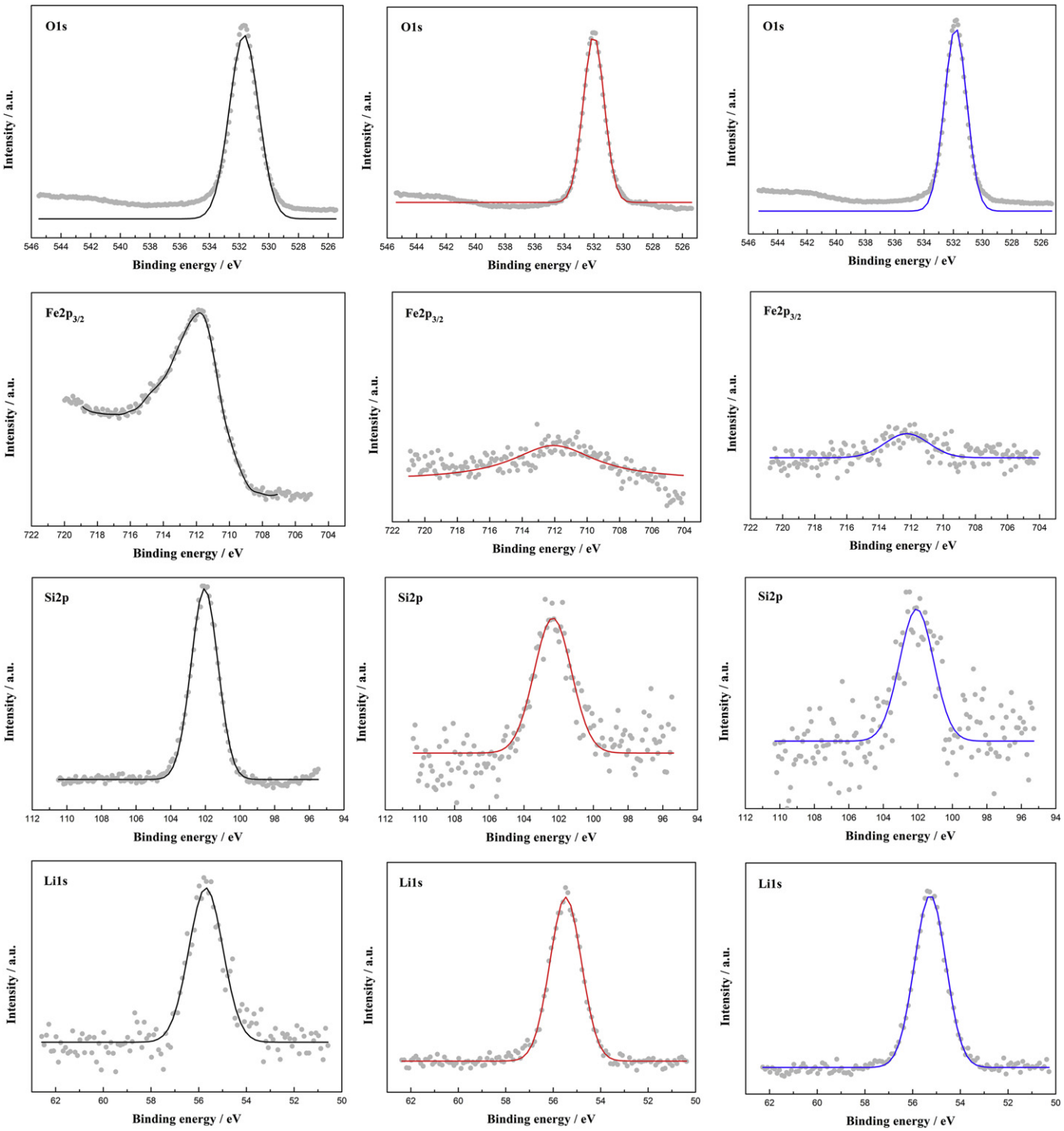

Fig. 5. XPS spectra for as-prepared Li_2FeSiO_4 (left column), Li_2FeSiO_4 electrode discharged to 0 V (middle column) and charged to 3.0 V (right column).

0 V, the crystalline peaks of the as-prepared Li_2FeSiO_4 disappeared, it converts to Fe, SiO_2 and Li_2O, the Li_2CO_3 is the outcome of reaction between Li_2O and CO_2 which exist in the ambient. Upon charged to 3 V, $LiFeO_2$ turns up along with SiO_2, Li_2O. There are no peaks of silicon in the diffractogram of materials discharged to 0 V and charged to 3.0 V. Although we can not unambiguously point out the reaction mechanism is, at least, it can be reliably believed that it is not Si-alloying mechanism. Li_2FeSiO_4 electrode can have such a high capacity, probably due to the $Fe^{3+}/Fe^{2+}/Fe^0$ redox reactions, which is similar to the mechanism reported by Poizot et al. [9].

XPS spectra for as-prepared Li_2FeSiO_4, Li_2FeSiO_4 electrode discharged to 0 V and charged to 3.0 V are shown in Fig. 5. It should be point out that the as-prepared Li_2FeSiO_4 sample and cycled electrode were exposed in air before XPS measurements. For as-prepared Li_2FeSiO_4, the strong peak at 531.37 eV in the O1s spectrum and the peak at 102.02 eV in the Si2p spectrum can be assigned to orthosilicate structure [SiO_4] [18]. For the electrode discharged to 0 V, the O1s peak at 532.01 eV, Li1s peak at 55.47 eV and Si2p peak at 102.31 eV can be expected for SiO_2, Li_2CO_3 [19–21]. For the electrode charged to 3 V, similar peaks can be detected. Because the escape depth of the ejected photoelectrons is only a few nanometers, the $Fe2p_{3/2}$ peak of cycled electrode is relatively weaken, it can be attributed to the screening effect of the Li_2CO_3 covered in the electrode surface. A peak at 711.82 eV can be found in the $Fe2p_{3/2}$ spectrum of the as-prepared Li_2FeSiO_4, which can be assigned to the Fe^{3+} in $LiFeSiO_4$. The absence of the peak at 709.8 eV for Fe^{2+} indicates that the surface of Li_2FeSiO_4 is entirely oxidized by atmospheric oxygen [14,19–21]. For the reason of surface contamination by air and moisture, the valence state of Fe is difficult to be accurately detected. The above results indicate that the valence states of Si, Li and O are not changed in the electrochemical reaction. Considering the high capacity of the anode material Li_2FeSiO_4, iron is the only promising element involving in the reaction of gain and loss electron.

To further investigate the electrochemical behavior and reaction mechanism, CV measurements were carried out with a scan rate of 0.2 mV s^{-1} in the potential range of 0–3.0 V (Fig. 6). In the first cathodic scan, a strong reduction peak at 0.68 V is observed, which can be associated with the initial reduction of Fe^{2+} to Fe^0 and the formation of the amorphous Li_2O; and the reduction peak at 0.12 V is related to the formation of the solid electrolyte interface (SEI) layer. In the first anodic scan, two overlapping broad peaks at ca. 1.6 and 2.0 V can observed, which can be assigned to a change in iron oxidation state in two steps (viz., Fe^0 to Fe^{2+} at ca. 1.6 V and Fe^{2+} to Fe^{3+} at ca. 2.0 V) [22]. However, the second curve is different from the first one, in which the reduction peaks become weaker, and shift to 0.8 and 1.3 V, which correspond to the reverse reaction. The subsequent CV curves are very similar to the second one, indicating the electrochemical reversibility of the electrodes is gradually built after the initial cycle and become much better [23]. These voltage values are bearing good resemblance to $LiFeO_2$ composites reported in the literature [24].

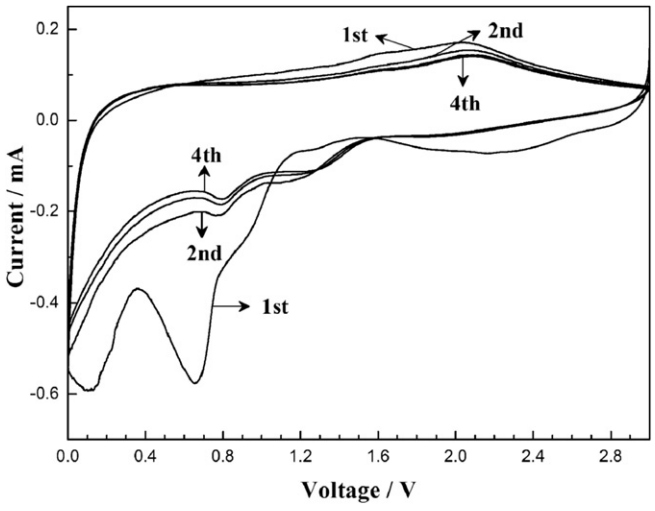

Fig. 6. Cyclic voltammograms of Li_2FeSiO_4 electrode at a scan rate of 0.2 mV s^{-1}.

4. Conclusions

Nanoparticle Li_2FeSiO_4 has been synthesized via sol–gel method and investigated systematically as an anode material for lithium ion batteries. The Li_2FeSiO_4 electrode exhibited an initial discharge capacity of 880 mA h g^{-1} at 50 mA g^{-1}, the discharge capacity retains 498 mA h g^{-1}after 30 cycles. *Ex-situ* XRD, XPS and cyclic voltammograms results shown that the electrochemical reaction isn't the Si-alloying mechanism. More detailed experiments (Mossbauer, XANES, etc.) are currently underway to identify the reaction mechanism. The extraordinarily performances, combined with the fact that raw materials are cheap, abundant and environmental benignity, make Li_2FeSiO_4 to be a suitably lithium battery anode material.

Acknowledgment

This work was supported by the Nature Science Foundation of China (No. 51104184 and No. 50972165).

References

[1] A.S. Arico, P.G. Bruce, B. Scrosati, J.M. Tarascon, W.V. Schalkwijk, Nat. Mater. 4 (2005) 366–377.
[2] H.J. Sohn, C.M. Park, J.H. Kim, H. Kim, Chem. Soc. Rev. 39 (2010) 3115–3141.
[3] X.J. Huang, H. Li, L.H. Shi, Q. Wang, L.Q. Chen, Solid State Ionics 148 (2002) 247–258.
[4] M.V. Reddy, T. Yu, C.H. Sow, Z.X. Shen, C.T. Lim, G.V.S. Rao, B.V.R. Chowdari, Adv. Funct. Mater. 17 (2007) 2792–2799.
[5] X.H. Huang, J.P. Tu, B. Zhang, C.Q. Zhang, Y. Li, Y.F. Yuan, H.M. Wu, J. Power Sources 161 (2006) 541–544.
[6] Q.M. Pan, L.M. Qin, J. Liu, H.B. Wang, Electrochim. Acta 55 (2010) 5780–5785.
[7] W.J. Zhang, J. Power Sources 196 (2011) 13–24.
[8] C.H. Chen, D.W. Zhang, S.Q. Zhang, Y. Jin, T.H. Yi, S. Xie, J. Alloys Compd. 415 (2006) 229–233.
[9] P. Poizot, S. Laruelle, S. Grugeon, L. Dupont, J.M. Tarascon, Nature 407 (2000) 496–499.
[10] N. Kalaiselvi, C.H. Doh, C.W. Park, S.I. Moon, M.S. Yun, Electrochem. Commun. 6 (2004) 1110–1113.
[11] D. Son, E. Kim, T.G. Kim, M.G. Kim, J.H. Cho, B. Park, Appl. Phys. Lett. 85 (2004) 5875–5877.
[12] Y.S. Lee, V. Aravindan, K. Karthikeyan, S. Amaresh, H.S. Kim, D.R. Chang, Ionics 17 (2011) 3–6.
[13] A. Nytén, A. Abouimrane, M. Armand, T. Gustafsson, J.O. Thomas, Electrochem. Commun. 7 (2005) 156–160.
[14] S. Zhang, C. Deng, B.L. Fu, S.Y. Yang, L. Ma, Electrochim. Acta 55 (2010) 8482–8489.
[15] S. Zhang, C. Deng, S.Y. Yang, Electrochem. Solid-State Lett. 12 (2009) A136–A139.
[16] T. Muraliganth, K.R. Stroukoff, A. Manthiram, Chem. Mater. 22 (2010) 5754–5761.
[17] S. Nishimura, S. Hayase, R. Kanno, M. Yashima, N. Nakayama, A. Yamada, J. Am. Chem. Soc. 130 (2008) 13212–13213.
[18] C. Satriano, E. Conte, G. Marletta, Langnmuir 17 (2001) 2243–2250.
[19] D. Ensling, M. Stjerndahl, A. Nytén, T. Gustafsson, J.O. Thomas, J. Mater. Chem. 19 (2009) 82–88.
[20] A. Nytén, M. Stjerndahl, H. Rensmo, H. Siegbahn, M. Armand, T. Gustafsson, K. Edström, J.O. Thomas, J. Mater. Chem. 16 (2006) 3484–3488.
[21] C. Deng, S. Zhang, Y. Gao, B. Wu, L. Ma, Y.H. Sun, B.L. Fu, Q. Wu, F.L. Liu, Electrochim. Acta 56 (2011) 7327–7333.
[22] J. Morales, L. Sánchez, F. Martín, F. Berry, X.L. Ren, J. Electrochem. Soc. 152 (2005) 1748–1754.
[23] X.Y. Xue, C.H. Ma, C.X. Cui, L.L. Xing, Solid State Sci. 13 (2011) 1526–1530.
[24] M.M. Rahmana, J.Z. Wang, M.F. Hassan, Z.X. Chen, H.K. Liu, J. Alloys Compd. 509 (2011) 5408–5413.